Polymer Bulletin (2020) 77:1929–1949
https://doi.org/10.1007/s00289-019-02831-x

ORIGINAL PAPER

Preparation of new PVC composite using green reduced graphene oxide and its effects in thermal and mechanical properties

Ferda Mindivan[1,3] · **Meryem Göktaş**[2,3]

Received: 4 November 2018 / Revised: 3 May 2019 / Accepted: 1 June 2019 / Published online: 14 June 2019

Abstract

In the present study, it was focused on developing mechanically stronger and thermally more stable polyvinyl chloride (PVC) composites by using green reduced graphene oxide (GRGO) filler to strengthen the negative features of PVC. For this purpose, GRGO reduced by vitamin C (ascorbic acid) with antibacterial properties was selected as filler. The PVC/GRGO composites were produced via colloidal blending method at different amounts of GRGO in PVC matrix (0.1, 0.3, 0.5 and 1% by weight), while pure PVC was also produced for comparison. The XRD and FTIR results showed that GRGO incorporated in the polymer matrix; this finding was also evident in SEM analysis. TGA and DSC analyses showed that the composite with 1% loading content of GRGO provided an important improvement on the thermal stability. The tensile strength and hardness of the composite having 0.1% GRGO increased by 42% and 98%, respectively. SEM image of PVC/GRGO-0.1 composite showed the galleries of GRGO filled with PVC. As a consequence, thermal and mechanical properties of PVC can be altered by changing loading content of GRGO. Moreover, the GRGO may be a good candidate for substitution of harmful fillers for PVC-based products.

Keywords Green reduced graphene oxide · PVC · Composite · Thermal properties · Mechanical properties

✉ Ferda Mindivan
ferda.mindivan@bilecik.edu.tr; ferdagtekin@hotmail.com

[1] Faculty of Engineering, Department of Bioengineering, Bilecik Seyh Edebali University, C Block, C240, Gülümbe Campus, 11230 Bilecik, Turkey

[2] Department of Metallurgy, Bilecik Seyh Edebali University, Vocational College, 11230 Bilecik, Turkey

[3] Bilecik Seyh Edebali University, Biotechnology Application and Research Center, 11230 Bilecik, Turkey

Introduction

Polyvinyl chloride (PVC) is a widely used thermoplastic of great technical and commercial importance [1, 2] since it is biocompatible, corrosion resistant, inert, versatile, durable and of low cost [3–5]. Today, the annual production volume of PVC is more than 35 million tones worldwide and PVC possesses the largest share of the medical market materials (blood bags, health-care devices, etc.) [1, 5, 6]. In addition, it has some additional application areas such as films, children's toys, food packaging, wall paper, bottle, flooring, roof tiles and electrical wire insulation [7–9]; however, its low thermal stability (heat distortion and relatively low softening temperatures) [3], inherent rigidity and poor mechanical properties limit its application areas [10, 11]. To extend its application area, PVC is commonly compounded with different amounts of additives (plasticizers, fillers or stabilizers) [5]. The most common additives are severely toxic, and they have negative effects on health [12]. Thus, there is a trend to use harmless additives, which reduce potential health and environmental hazards [13]. Graphene and graphene derivatives such as graphene oxide (GO), reduced graphene oxide (RGO), modified graphene oxide, multilayer graphene (MLG) and graphene nanoplates (GNPs) are widely used as fillers for composites [14]. Pristine graphene is hydrophobic [15] and does not disperse well in polymer matrix [16]. The dispersion of the fillers within the polymer matrix is important to form intercalated or exfoliated composites and to enhance various properties of the composite materials [17]. GO and RGO as inexpensive filler materials are used to produce polymer composites because of their easy synthesis, large surface areas and layered structures [18–21]. GO is hydrophilic and contains epoxy, alcohol, carbonyl and carboxyl groups, and the RGO sheets have alcohol and carboxyl groups [22]. Thus, GO and RGO are used to settle dispersion problem [23]. At the same time, they have emerged as a new antibacterial material because of their less cytotoxicity toward mammalian cells [24, 25] and they were often used for biomedical applications. The antibacterial activity of GO and RGO was reported by many researchers [26–28]. For instance, Hu et al. [26] have evaluated the cellular uptake and cytotoxicity of GO and RGO nanosheets and showed that graphene-based nanomaterials have found to be excellent antibacterial material with mild cytotoxicity due to different surface charges and functional groups of GO and RGO nanosheet surfaces. Also, Liu et al. [28] have investigated the antibacterial activity of four types of graphene-based materials (graphite, graphite oxide, GO and RGO) and found that the physicochemical properties (the density of functional groups, size and conductivity) of these materials can affect the antibacterial behavior. Solution-based chemical reduction is the most widely used that of among several methods to produce RGO [29]. Unfortunately, highly toxic nature and instability of the reducing agents (hydrazine hydrate, dimethyl hydrazine, hydroquinone, sodium borohydride, metal hydrides) give the reduction process of GO a negative aspect [30, 31]. Recently, nontoxic or natural products such as non-aromatic amino acids [32], leaf extracts of natural products [30], ethylene glycol [33], sodium carbonate [23], sugar [34] and green tea [35] have offered

environmentally friendly approaches to reduce GO [36, 37]. In our study, to this aim, we choose a green method in which GO is prepared from graphite by Hummers method and then reduced by vitamin C to obtain green reduced graphene oxide (GRGO). It is an eco-friendly reducing agent with antioxidant properties [38, 39]. There are several studies conducted to improve thermal, chemical and mechanical properties of PVC composites by using graphene derivatives [10, 11, 40, 41]. Deshmukh et al. [10] have prepared PVC/GO composite films by using colloidal blending method, and they investigated surface properties of these composites. Hu et al. [11] have examined the properties of GO and RGO modified with polydopamine- and poly(methyl methacrylate)-filled PVC nanocomposite films. In their study, they reported that the improvement of mechanical and thermal properties was depended on the interfacial interactions. Yassin et al. have reported the adjustable structural, optical, electrical and thermal properties of polymer matrix nanocomposites with the different GO concentrations. They found that the homogeneous and well-dispersed GO had helped in the significant enhancement of the different properties of the composite [40]. Among the GO and RGO filler studies, to the best of our knowledge, there are no report on the green synthesis of graphene-based fillers for PVC and their effects on the mechanical properties of PVC composites, in the literature. The objective of this work is to produce a good candidate for the substitute of harmful or toxic fillers for PVC composites and to investigate the thermal and mechanical properties of PVC/GRGO composites which can be used for manufacturing of toys, baby products and biomedical products.

Materials and methods

Materials

Natural graphite (45 μm nominal particle size) powder (GF), concentrated sulfuric acid (98% H_2SO_4), potassium permanganate ($KMnO_4$), hydrogen peroxide (30% H_2O_2) solution, hydrochloric acid (HCI), tetrahydrofuran (THF) and vitamin C [L(+)-Ascorbic Acid] were of reagent grade and purchased from Merck. All the reagents were used without further purification. All solutions were prepared using deionized (DI) water.

GO synthesis

GO was prepared from the GF by the Hummers method [42]. GF (1 g) was mixed with 69 mL of concentrated H_2SO_4, and the mixture was stirred in an ice bath for around 30 min. After homogeneous dispersion of the GF in the solution is obtained, $KMnO_4$ (8 g) was added slowly to the solution and the reaction mixture was stirred for 15 min. Then, the ice bath was removed and the mixture was stirred at 35 °C overnight until obtaining a thick paste. Afterward, 70 mL of deionized (DI) water was added slowly into the reaction solution to avoid the reaction temperature rising

to a limit of 98 °C. After 2 h of vigorous stirring, 12 mL of 30% H_2O_2 was added and the color turned golden yellow immediately. Finally, the mixture was then filtered and washed several times with 3% HCl and DI water and dried at 65 °C for 12 h.

GRGO synthesis

To prepare GRGO, 0.5 g of GO was dispersed in 100 mL of DI water. pH of the GO suspension was adjusted to ~ 10 by using ammonia solution. Then 0.75 g of vitamin C was added to the mixture and reaction medium was held at 95 °C for 12 h. After that the mixture was filtered and the GRGO was obtained as a black powder. This powder was washed with DI water several times.

Preparation of PVC/GRGO composites

PVC/GRGO composites were prepared by a colloidal blending method. PVC (1 g) was first dissolved in THF at 70 °C and was cooled to room temperature. GRGO powder was separately dispersed in THF at 25 °C. These mixtures were then added in another flask, and this mixture was stirred for 2 h at 60 °C. The resulting homogeneous dispersion was poured into glass petri dish and kept in an oven at 60 °C for slow evaporation of the solvent to get PVC/GRGO composites. The synthesis process of GRGO sample and PVC/GRGO composites is illustrated in Fig. 1. The GRGO content in the PVC/GRGO composite was varied between 0.1 and 1% by weight. A series of PVC/GRGO composites were prepared and coded as PVC/GRGO-0.1, PVC/GRGO-0.3, PVC/GRGO-0.5 and PVC/GRGO-1 according to their GRGO content.

Characterization of GRGO sample and PVC/GRGO composites

Chemical and structural characterization of the GRGO and PVC/GRGO composites were carried out by FTIR analysis (Spectrum 100, Perkin Elmer), between 4000 and 400 cm^{-1} and X-Ray diffraction analysis (XRD, PAN analytical, Empyrean) between 5° and 50°of 2θ. The surface morphology was examined by scanning electron microscopy (SEM, Supra 40VP, Zeiss). EDS analysis were performed on the same instrument. Thermogravimetric analysis (TGA, STA 409, Netzsch) was performed by heating the samples from 20 to 600 °C at a rate of 10 °C min^{-1} in a nitrogen atmosphere. Differential scanning calorimetry (DSC, STA 409, Netzsch) analysis was performed by heating the samples from 20 to 600 °C. The tensile test samples with a gage length of 80 mm were also tested according to the ASTM D 3822 standard [43] on Lloyd LR 5 K tensile testing machine with a load cell of 10 N and the deformation rate of 20 mm/min. All tensile test results were presented as an average value of five tests with standard deviations. Microhardness measurement was carried out on a metallographic sample under the load of 10 g with a Knoop indenter. At least ten successive measurements were performed for each condition.

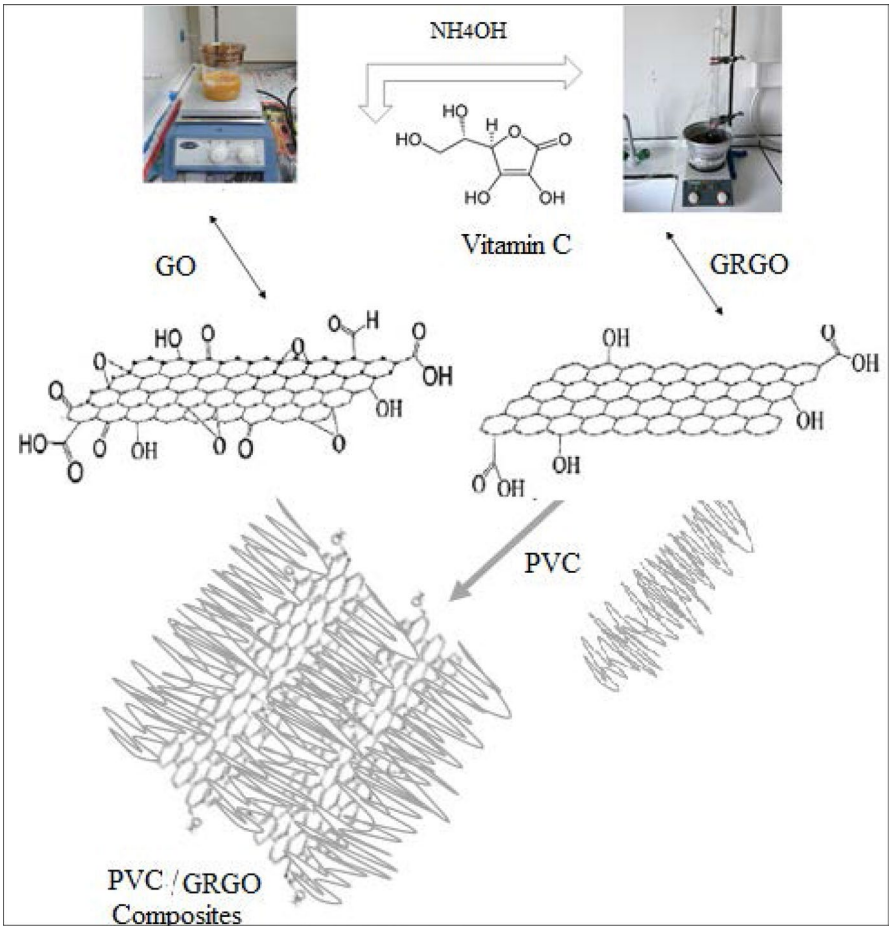

Fig. 1 Illustration for the preparation of GRGO sample and PVC/GRGO composites

Results and discussion

FTIR analysis

FTIR spectra of the GO and GRGO samples are shown in Fig. 2. The FTIR spectra of GO in Fig. 2 confirms the presence of functional groups such as hydroxyl (O–H), carbonyl (C=O), carboxylic acid (C–OH) and epoxy groups (C–O) of GO. FTIR spectra of GO shows characteristic peaks which are at 3214 cm^{-1} O–H vibration of the adsorbed water [44, 45], at 1723 cm^{-1} (C=O stretch of carbonyl groups) [46], at 1392 cm^{-1} (C–OH stretch) [47] and at 1207–1043 cm^{-1} (C–OH and C–O bonds of carboxylic acid and epoxy groups) [47, 48]. These results confirm the oxygen-containing functional groups of the GO. The FTIR spectra of the GRGO, by the way, shows a decrease in the intensity of alcohol and carbonyl

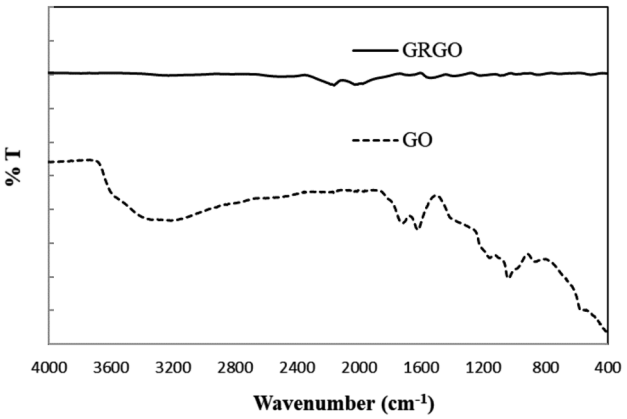

Fig. 2 FTIR spectra of GO and GRGO samples

group peaks by comparison with GO (Fig. 2). In addition to that, the intensities of carboxylic acid-epoxy groups of GO were almost disappeared in the FTIR spectra of the GRGO. These results indicated that GO was successfully reduced by vitamin C according to removal of oxide functional groups [22]. As shown in Fig. 3, FTIR spectra of PVC/GRGO has characteristic peaks at 2911 cm^{-1} and 2859 cm^{-1}, corresponding to C–H stretching and vibration peaks, respectively. For PVC/GRGO composites, the characteristic CH_2 stretching and vibration peaks were observed at 1426 cm^{-1}. The peaks at 1252 cm^{-1} and 956 cm^{-1} were assigned to CH-rocking and trans CH wagging vibration, respectively. The stretching peak of C–Cl was observed at 834 cm^{-1}, and the peak at 611 cm^{-1} was assigned to *cis* CH wagging vibration [49]. As seen from Fig. 3, intensities of all characteristic peaks corresponding to PVC structure decrease with the increase in GRGO loading content. This result indicates GRGO loading in the polymer

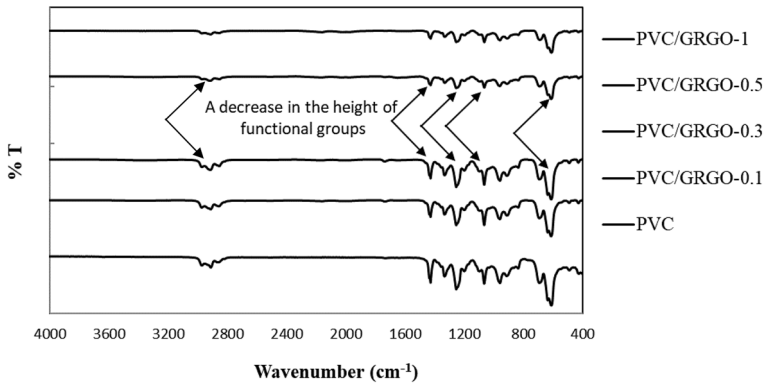

Fig. 3 FTIR spectra of pure PVC and PVC/GRGO composites

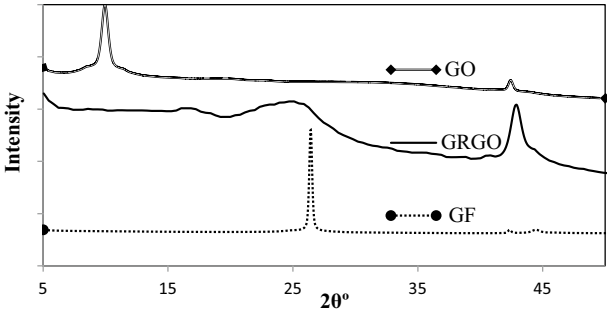

Fig. 4 X-ray diffraction patterns of GF, GO and GRGO samples

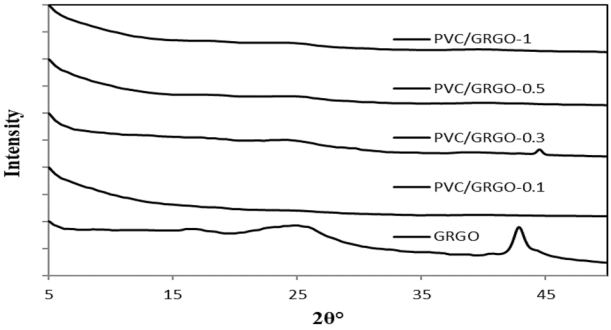

Fig. 5 X-ray diffraction patterns of GRGO sample and PVC/GRGO composites

matrix is accomplished, because of diminished vibration intensities with the increment in GRGO content.

XRD analysis

XRD patterns of GF, GO and GRGO samples are presented in Fig. 4. The diffraction peak of crystalline GF was found at $2\theta^\circ = 26.4^\circ$. The interlayer distance of GF was 0.337 nm. GO exhibited a sharp peak at $2\theta^\circ = 9.95^\circ$ corresponding to the (002) plane of GO and inter-planner spacing of 0.888 nm. These results demonstrated that successful synthesis of the GO from GF by the Hummers method [50] and the interlayer distance increased from 0.337 to 0.888 nm. The oxygen-containing functional groups are responsible for the increase in the interlayer distance [51, 52]. GRGO had a broad peak that appears at $2\theta^\circ = 24.04^\circ$, while the characteristic peak of GO at $2\theta^\circ = 9.95^\circ$ was disappear. This indicated reduction of GO by vitamin C (Fig. 4) [53, 54]. PVC/GRGO composites, however, have no peak in their XRD patterns (Fig. 5) due to their amorphous nature [55] and uniform dispersion of GRGO in the PVC matrix. These results confirm the intercalated structure of PVC/GRGO composites.

SEM analysis

Figure 6a, b shows microstructure of the GO and GRGO samples, respectively. In the SEM image of GO before reduction (Fig. 6a), a randomly aggregated morphology of GO can be seen [56, 57]. Figure 6b which is the magnified SEM image of GRGO shows a wrinkle-like structure due to the rapid removal of hydroxyl, carbonyl and epoxy groups of GO [58]. The oxygen content atom percentages can be considered as a measure of the GO that was reduced, because of the EDS analysis provides the elemental content information. Oxygen content of the GRGO was 24.03%, while GO was 46.78% as shown in Table 1. This result also strengthens the evidence of

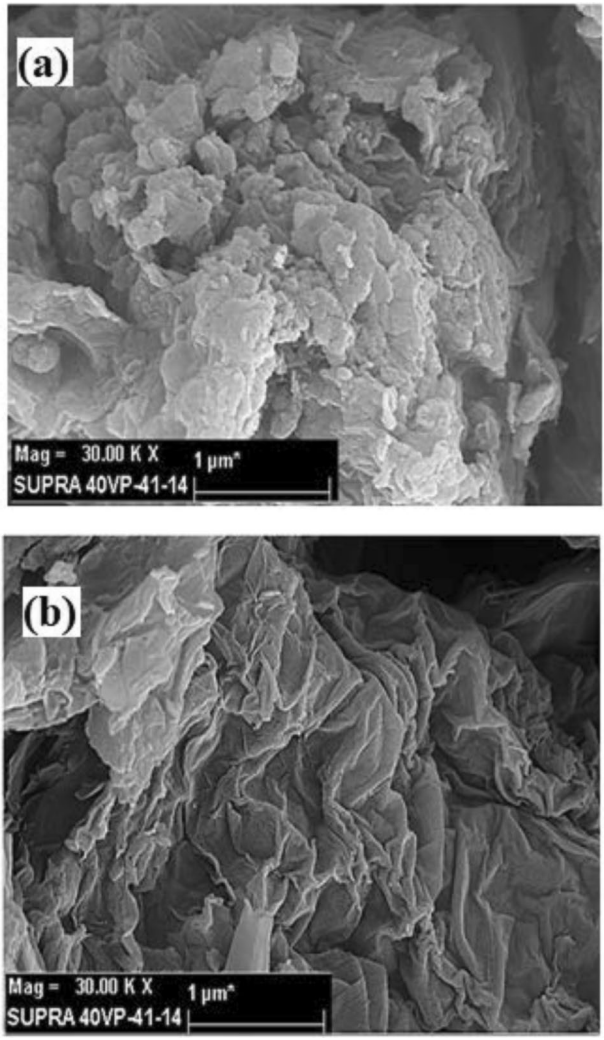

Fig. 6 SEM images of **a** GO, **b** GRGO samples (magnification 30.000 KX)

Table 1 EDS results of GO and GRGO samples

Samples	EDS
GO	Element Series unn. C [wt.%] norm. C [wt.%] Atom. C [at.%] Error (1 Sigma) [wt.%] Carbon K-series 46.07 46.07 53.22 8.85 Oxygen K-series 53.93 53.93 46.78 10.70 Total: 100.00 100.00 100.00
GRGO	Element Series unn. C [wt.%] norm. C [wt.%] Atom. C [at.%] Error (1 Sigma) [wt.%] Carbon K-series 70.37 70.37 75.98 11.73 Oxygen K-series 29.63 29.63 24.02 7.60 Total: 100.00 100.00 100.00

successful GO reduction. The results obtained from the FTIR are compatible with EDS results. Figures 7 and 8 present the SEM images of the surfaces and fracture cross section of pure PVC and PVC/GRGO composites, respectively. Figure 7a shows the pure PVC surface was smooth and has no signs of pits or pores. It could be seen that the fracture surface of pure PVC was relatively flat (Fig. 8a, b). Figure 7b exhibits the PVC composite with 0.1% GRGO was irregular and bumpy with a rough surface owing to polymer growing in the galleries of GRGO [59]. White regions in the SEM images corresponding to PVC can be clearly observed in the pits (see dashed circles in Fig. 7b). A high-magnification SEM image of PVC/GRGO-0.1 composite shows that GRGO and PVC had good compatibility and the galleries of GRGO filled with PVC (see the black arrows in Fig. 7b1). Furthermore, as the content of GRGO increased to 0.1%, the morphology of the fracture surface was totally different and the layers stacked in a more compact manner (Fig. 8b, b1). The PVC/GRGO-0.1 composite gave better dispersion with no agglomeration, and this gave better increase in mechanical properties compared with other samples (0.3, 0.5 and 1% by weight). The PVC/GRGO-0.5 composite exhibited less bumpy but more deep pits than the PVC/GRGO-0.3 composite (Fig. 7c, d) because the number of deep pits increased with an increase in GRGO content. A high-magnification SEM image of PVC/GRGO-0.5 composite (Fig. 7d1) shows deep pits because enough polymer entering the galleries of GRGO was not found. When the GRGO content was 0.5%, the corresponding fracture surface was same as 0.1% and the GRGO were homogeneously distributed within the polymer matrix (Fig. 8d, d1). From the SEM image of the PVC composite with 1% GRGO (Fig. 7e), it could be seen that the number

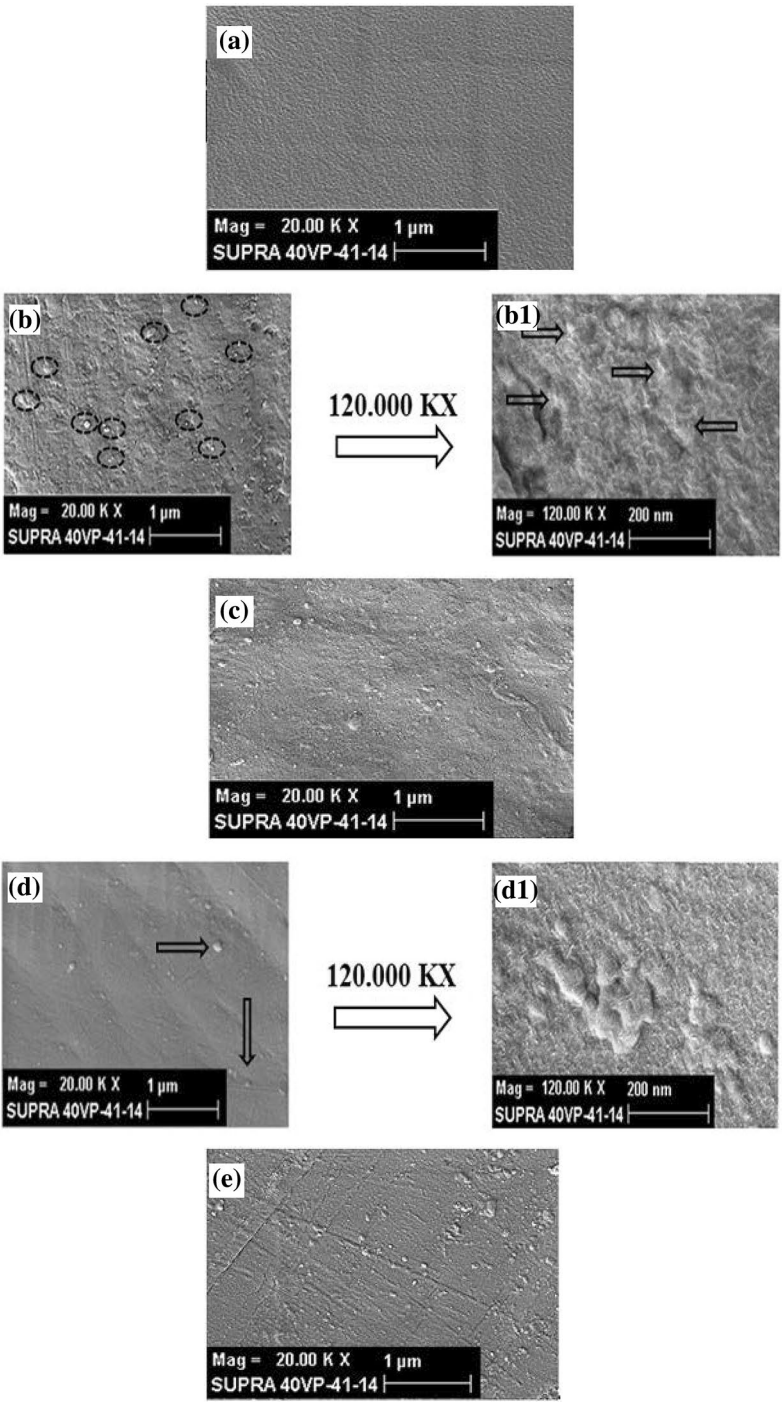

Fig. 7 SEM images of **a** pure PVC, **b** PVC/GRGO-0.1, **c** PVC/GRGO-0.3, **d** PVC/GRGO-0.5, **e** PVC/GRGO-1(magnification 20.00 KX), **b1** PVC/GRGO-0.1 and **d1** PVC/GRGO-0.5 (magnification 120.00 KX)

of pits increased. As the content of GRGO was 0.3 and 1.0%, the corresponding fracture surface is uneven and layered (Fig. 8c, c1, e, e1). Undoubtedly, the GRGO loading amount will lead to different mechanical behaviors, which will be discussed in mechanical properties section.

DSC analysis

Figure 9 shows the differential scanning calorimetry (DSC) thermograms and melting points of pure PVC and PVC/GRGO composites. Melting point of the pure PVC was observed at 297.90 °C. DSC curves of PVC/GRGO-0.1, PVC/GRGO-0.3, PVC/GRGO-0.5 and PVC/GRGO-1 showed a correlated degradation peak centered at 279.47 °C, 269.39 °C, 274.42 °C and 284.51 °C, respectively (Fig. 9). It could be seen that the melting point of pure PVC was shifted to a lower temperature with the GRGO loading. The reason could be attributed to the extensive effect of the addition of fillers because GRGO restricted polymer chain movement by H-bonding between hydroxyl groups on the edges of GRGO and the hydrogen groups of PVC chains [60–62]. As shown in Fig. 9, the melting point peaks of all composites both shifted to lower temperatures and became broad with the increase in GRGO content. The broad melting transition peak was concerned interaction between GRGO and PVC [63]. Moreover, the PVC/GRGO composite with the maximum GRGO content (1%) showed the highest melting point (284.51 °C). The PVC/GRGO-1 composite typically had the best thermal stability among the other composites used in this study [64, 65].

TGA analysis

TGA weight loss and derivative thermograms (DTG) for the PVC/GRGO composites with different GRGO content are given in Fig. 10, and thermal parameters are summarized in Table 2. PVC and its composites showed two and three stages of decomposition, respectively (T_1, T_2 and T_3). The first decomposition temperature (T_1) was observed in 172 °C for the pure PVC, corresponding to the loss of water from the chains of polymer. T_1 temperatures of the PVC/GRGO-0.1, PVC/GRGO-0.3, PVC/GRGO-0.5 and PVC/GRGO-1 composites were about the same (Table 2). Composites showed much lower T_1 temperatures than pure PVC because the GRGO and PVC interaction facilitated the removal of water from the structure [60, 66]. The main decomposition temperatures (T_2) were observed at 296 °C for pure PVC and between 285 and 288 °C for all composites (Table 2). The step in T_2 temperature (285–288 °C) can be attributed to the emission of HCl according the degradation of both pure PVC and PVC/GRGO composites [67, 68]. C–Cl bonds are unstable in PVC at T_2 temperature, and OH groups of GRGO attract to C–Cl unstable bonds in PVC. Cl is separated from C–Cl bond and the appearing of Cl radical. Cl radical takes a hydrogen from C–H bond, and HCl molecule leaves the polyene backbone [59, 62, 69]. T_2 temperature of the PVC/GRGO-1 composite was higher than all PVC/GRGO composites. PVC/GRGO-1 provided better thermal stability than other PVC/GRGO composites. TGA analysis results were in good agreement with

Fig. 8 SEM images of fracture surfaces of **a** pure PVC, **b** PVC/GRGO-0.1, **c** PVC/GRGO-0.3, **d** PVC/GRGO-0.5, **e** PVC/GRGO-1(magnification 250 X), **a1** pure PVC **b1** PVC/GRGO-0.1, **c1** PVC/GRGO-0.3, **d1** PVC/GRGO-0.5 and **e1** PVC/GRGO-1 (magnification 10.00 KX)

that obtained from DSC (Fig. 9). Moreover, an increase in the third decomposition temperatures (T_3) for PVC/GRGO composites compared to pure PVC was observed (Table 2). Thermal degradation of the composites was observed at this stage, resulting in the formation of volatile aromatic compounds and a stable carbonaceous residue [70, 71]. As shown in Table 2, the weight loss of PVC/GRGO-1 composite was lower than the other PVC/GRGO composites which indicated that the dispersion of GRGO hinders the formation of volatile aromatic compounds along with an increase in carbonaceous residue [62]. The TGA results were consistent with the results obtained from DSC and XRD studies. DSC and XRD results showed that there was interaction between fillers and polymer matrix because GRGO was homogeneously dispersed in the PVC matrix.

Mechanical properties

Mechanical properties of PVC/GRGO composites were characterized by their tensile strength, elongation at break and hardness. The effects of GRGO loading content on tensile strength of the PVC/GRGO composites are shown in Fig. 11. Tensile strength of all PVC/GRGO composites was higher than pure PVC. However, tensile strength of PVC/GRGO composites decreased with an increase in GRGO contents. Tensile strength of the PVC/GRGO-0.1 increased by 42%, compared with that of pure PVC. SEM images confirmed the presence of PVC filling the galleries of GRGO in the PVC/GRGO-0.1 composite (Fig. 8b, b1). The influences of GRGO loading content on elongation at break and hardness of the PVC/GRGO composites are presented in Figs. 12 and 13, respectively. As seen from Fig. 12, compared to pure PVC, PVC/GRGO composites have had lower elongation at break. Zheng et al. [72] have reported that the decrease in elongation at break for PVC composites might be due to high brittleness. This result was in accordance with our results. However, hardness of the PVC/GRGO composites increased at all GRGO loading content (Fig. 13) and when the loading content is 0.1%, the value increased by 98% in contrast to that of pure PVC. The distribution of GRGO in PVC matrix, as discussed in thermal analysis and XRD sections, may result in an increase in resistance to indentation. Accordingly, the hardness of the composites increased at all GRGO loading content, because under the effect of external force, the uniform dispersion of filled phase in the composite can hinder the movement of dislocations which contribute to the improved hardness of the composites [73]. The rigid structure of the materials also partially contributes to the increase in hardness. According to the literature, there is a relationship between hardness and rigidity of composites [74]. Crespo et al. [74] experimentally examined the degree of influence of filler amount in PVC composites. They have reported the increased rigidity of the PVC composite that was accompanied with increase in hardness and tensile module. Results of mechanical characterization revealed that the incorporation of GRGO could improve

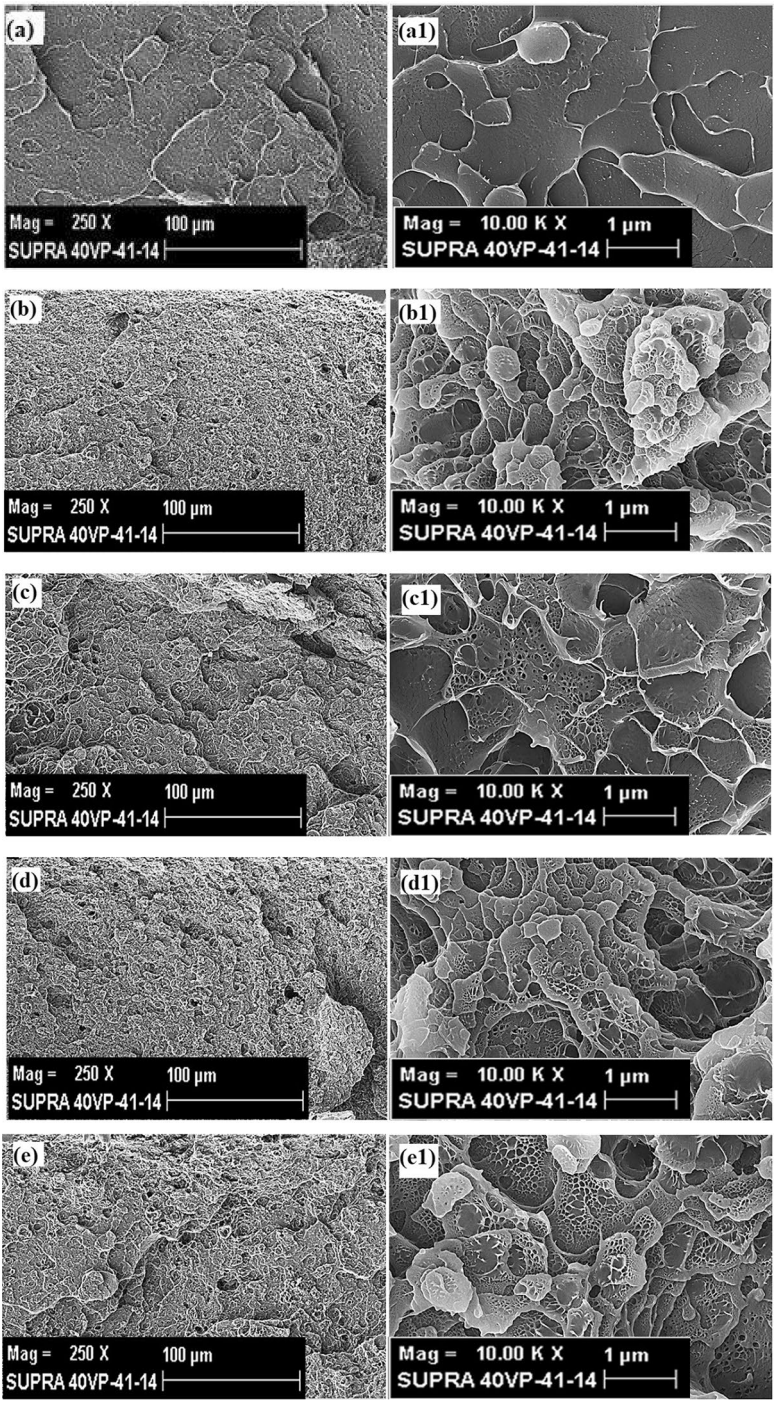
(a)
Mag = 250 X 100 µm
SUPRA 40VP-41-14
(a1)
Mag = 10.00 K X 1 µm
SUPRA 40VP-41-14
(b)
Mag = 250 X 100 µm
SUPRA 40VP-41-14
(b1)
Mag = 10.00 K X 1 µm
SUPRA 40VP-41-14
(c)
Mag = 250 X 100 µm
SUPRA 40VP-41-14
(c1)
Mag = 10.00 K X 1 µm
SUPRA 40VP-41-14
(d)
Mag = 250 X 100 µm
SUPRA 40VP-41-14
(d1)
Mag = 10.00 K X 1 µm
SUPRA 40VP-41-14
(e)
Mag = 250 X 100 µm
SUPRA 40VP-41-14
(e1)
Mag = 10.00 K X 1 µm
SUPRA 40VP-41-14

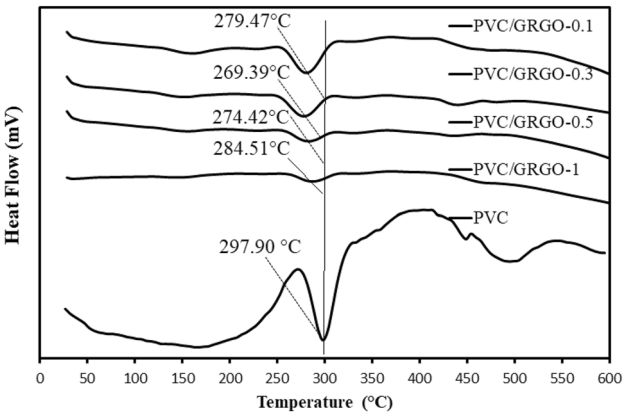

Fig. 9 DSC curves of the pure PVC and PVC/GRGO composites

the strength and GRGO galleries filled with PVC at the lowest loading content, but increased brittleness in the PVC/GRGO composites.

Conclusions

The effects of GRGO on mechanical and thermal properties of PVC were studied. The following conclusions can be drawn from the results of this study.

- FTIR results showed that there was interaction between the GRGO and PVC. It could be affirmed the good dispersion of the GRGO samples in the PVC matrix as confirmed by XRD analysis.
- The SEM image confirmed the presence of PVC filling in the galleries of GRGO (for instance, PVC/GRGO-0.1 composite). The number of deep pits increased with the increase in GRGO loading contents, and enough polymer entering the galleries of GRGO was not found in PVC/GRGO-0.3, 0.5 and 1 composites.
- TGA and DSC analyses showed that the PVC/GRGO-1 composite provide an important improvement on the thermal stability in comparison with that of other composites.
- The tensile strength and hardness of the PVC/GRGO-0.1 composite 42% and 98% higher, respectively, than the pure PVC.
- According to thermal and mechanical analysis results, the loading content of GRGO can be varied to change desired thermal and mechanical properties.
- Consequently, the GRGO is a good candidate for replacement of harmful/toxic fillers in the production of PVC, for instance used in toys, baby products and biomedical products.

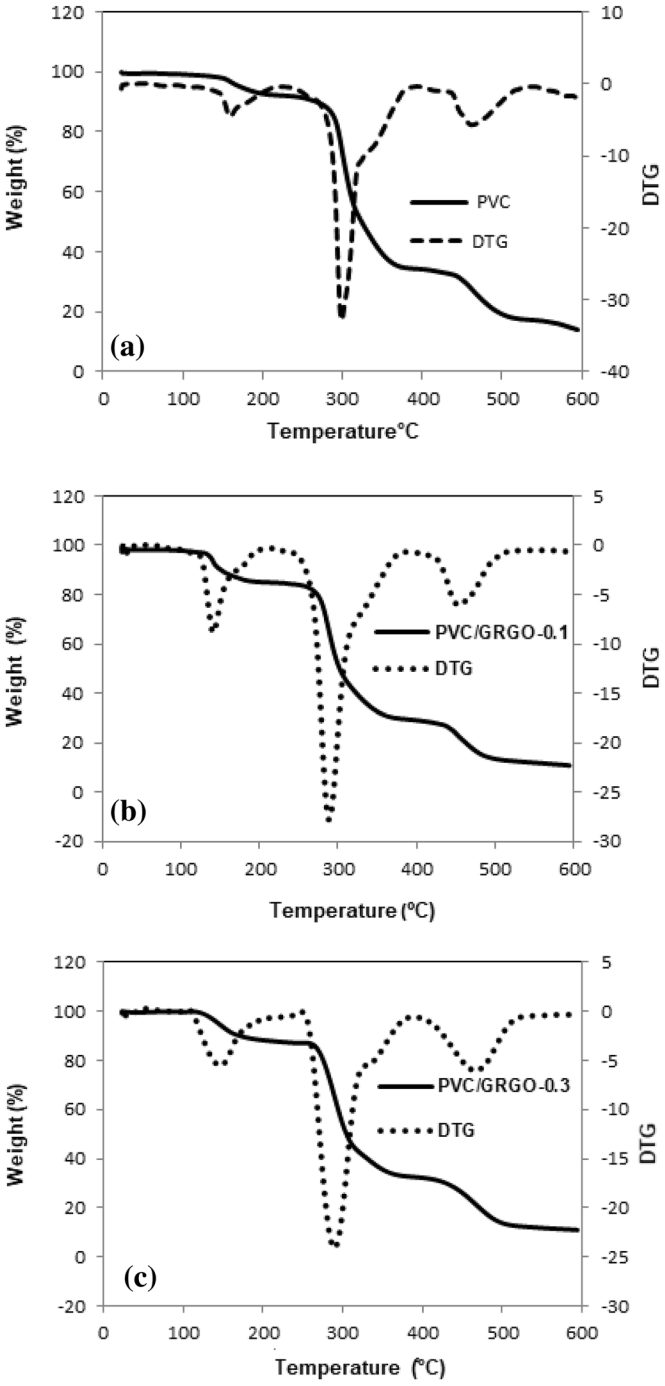

Fig. 10 TGA and DTG curves of **a** pure PVC, **b** PVC/GRGO-0.1, **c** PVC/GRGO-0.3, **d** PVC/GRGO-0.5 and **e** PVC/GRGO-1

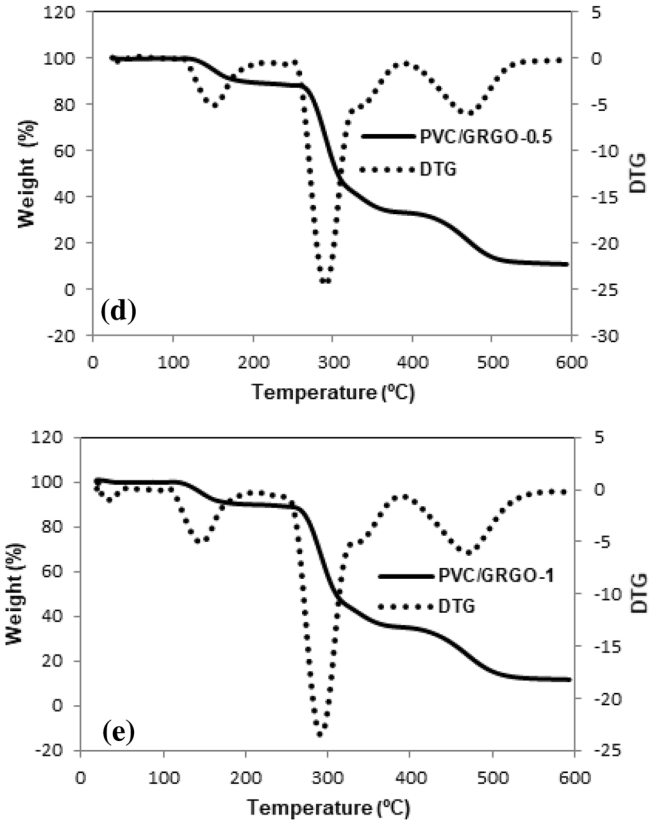

Fig. 10 (continued)

Table 2 Thermal parameters for the PVC/GRGO composites (10 °C/min heating rate, under nitrogen atmosphere)

Samples	T (°C) range			Weight loss at 600 °C (%)	Residue at 600 °C wt (%)
	T_1	T_2	T_3		
PVC	–	296	453	72.40	27.60
PVC/GRGO-0.1	138	286	447	89.12	10.88
PVC/GRGO-0.3	137	285	457	88.93	11.07
PVC/GRGO-0.5	140	287	457	89.07	10.93
PVC/GRGO-1	139	288	459	88.26	11.74

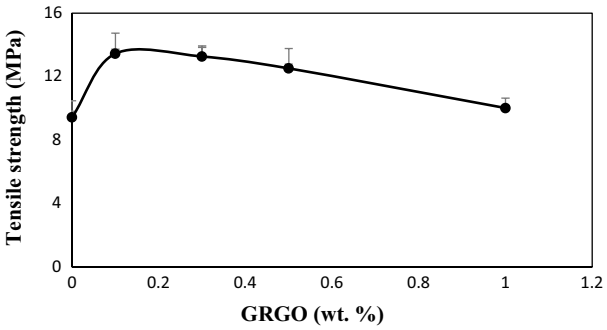

Fig. 11 The tensile strength of the PVC/GRGO composites with different contents of GRGO

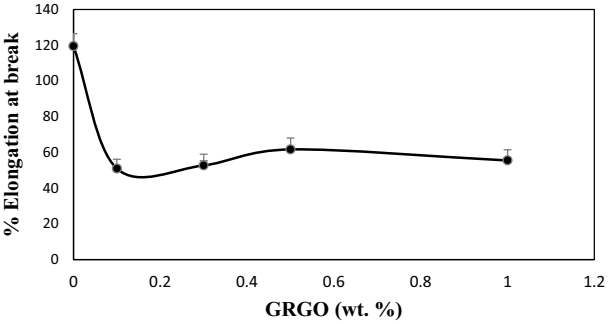

Fig. 12 The elongation at break of the PVC/GRGO composites with different contents of GRGO

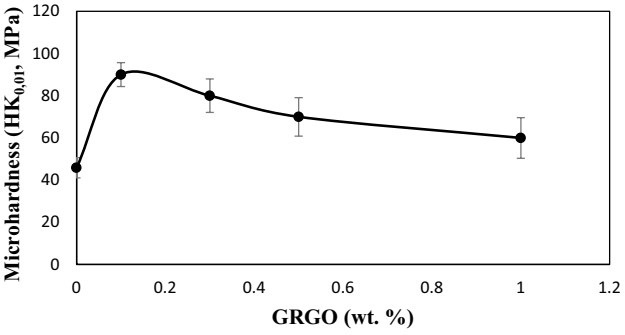

Fig. 13 The microhardness of the PVC/GRGO composites with different contents of GRGO

Acknowledgements The authors thank the financial support of the research foundation (Project No: 2015-02.BSEU.07-01) of Bilecik Seyh Edebali University.

Compliance with ethical standards

Conflict of interest The authors declare that they have no conflict of interest.

References

1. Wang K, He Y, Song X, Cui X (2015) Effects of the metakaolin-based geopolymer on high-temperature performances of geopolymer/PVC composite materials. Appl Clay Sci 114:586–592
2. Dan-asabe B (2016) Thermo-mechanical characterization of banana particulate reinforced PVC composite as piping material. JKSUES 223:1–9
3. Mallakpour S, Darvishzadeh M (2018) Nanocomposite materials based on poly(vinyl chloride) and bovine serum albumin modified ZnO through ultrasonic irradiation as a green technique: optical, thermal, mechanical and morphological properties. Ultrason Sonochem 41:85–99
4. Suzuki AH, Botelho BG, Oliveira LS, Franca AS (2018) Sustainable synthesis of epoxidized waste cooking oil and its application as a plasticizer for polyvinyl chloride films. Eur Polym J 99:142–149
5. Chiellini F, Ferri M, Morelli A, Dipaola L, Latini G (2013) Perspectives on alternatives to phthalate plasticized poly(vinyl chloride) in medical devices applications. Prog Polym Sci 38:1047–1088
6. Fang Y, Wang Q, Guo C, Song Y, Cooper PA (2013) Effect of zinc borate and wood flour on thermal degradation and fire retardancy of Polyvinyl chloride (PVC) composites. J Anal Appl Pyrol 100:230–236
7. Chen X, Li C, Zhang L, Xu S, Zhou Q, Zhu Y, Qu X (2004) Main factors in preparation of antibacterial particles/PVC composite. China Part 2(5):226–229
8. Janajreh I, Alshrah M, Zamzam S (2015) Mechanical recycling of PVC plastic waste streams from cableindustry: a case study. Sustain Cities Soc 18:13–20
9. Hakkarainen M (2003) New PVC materials for medical applications—the release profile of PVC/polycaprolactone–polycarbonate aged in aqueous environments. Polym Degrad Stab 80:451–458
10. Deshmukh K, Khatake SM, Joshi GM (2013) Surface properties of graphene oxide reinforced polyvinyl chloride nanocomposites. J Polym Res 20(286):1–11
11. Hu J, Jia X, Li C, Ma Z, Zhang G, Sheng W, Zhang X, Wei Z (2014) Effect of interfacial interaction between graphene oxide derivatives and poly(vinyl chloride) upon the mechanical properties of their nanocomposites. J Mater Sci 49:2943–2951
12. Brostow W, Lu X, Osmanson AT (2018) Nontoxic bio-plasticizers for PVC as replacements for conventional toxic plasticizers. Polym Test 69:63–70
13. Arrieta MP, Samper MD, Jiménez-López M, Aldas M, López J (2017) Combined effect of linseed oil and gum rosin as natural additives for PVC. Ind Crops Prod 99:196–204
14. Mindivan F (2015) The synthesis, thermal and structural characterization of polyvinylchloride/graphene oxide (PVC/GO) composites. Mater Sci Non-Equilib Phase Transform 3:33–36
15. Li J, Miao D, Yang R, Qu L, Harrington PB (2014) Synthesis of poly (sodium 4-styrenesulfonate) functionalized graphene/cetyltrimethylammonium bromide (CTAB) nanocomposite and its application in electrochemical oxidation of 2,4-dichlorophenol. Electrochim Acta 125:1–8
16. Kuila T, Khanra P, Mishra AK, Kim NH, Lee JH (2012) Functionalized-graphene/ethylene vinyl acetate co-polymer composites for improved mechanical and thermal properties. Polym Testing 31:282–289
17. Mindivan F (2017) Effect of various initial concentrations of CTAB on the noncovalent modified graphene oxide (MGNO) structure and thermal stability. Mater Testing 9(59):729–734
18. Kim F, Cote LJ, Huang J (2010) Graphene oxide: surface activity and two-dimensional assembly. Adv Mater 22:1954–1958
19. Veerapandian M, Lee M-H, Krishnamoorthy K, Yun K (2012) Synthesis, characterization and electrochemical properties of functionalized graphene oxide. Carbon 50:4228–4238

20. Stankovich S, Dikin DA, Piner RD, Kohlhaas KA, Kleinhammes A, Jia Y, Wu Y, Nguyen ST, Ruoff RS (2007) Synthesis of graphene-based nanosheets via chemical reduction of exfoliated graphite oxide. Carbon 45:1558–1565
21. Park S, An J, Jung I, Piner RD, An SJ, Li X, Velamakanni A, Ruoff RS (2009) Colloidal suspensions of highly reduced graphene oxide in a wide variety of organic solvents. Nano Lett 9(4):1593–1597
22. Singh V, Joung D, Lei Z, Das S, Khondaker SI, Seal S (2011) Graphene based materials: past, present and future. Prog Mater Sci 56:1178–1271
23. Jin Y, Huang S, Zhang M, Jia M, Hu D (2013) Green and efficient method to produce graphene for electrochemical capacitors from graphene oxide using sodium carbonate as a reducing agent. Appl Surf Sci 268:541–546
24. Sandhya PK, Jose J, Sreekala MS, Padmanabhan M, Kalarikkal N (2018) Reduced graphene oxide and ZnO decorated graphene for biomedical applications. Ceram Int 44:15092–15098
25. Maddinedi SB, Sonamuthu J, Suzuk Yıldız S, Han G, Cai Y, Gao J, Ni Q, Yao J (2018) Silk sericin induced fabrication of reduced graphene oxide and its in vitro cytotoxicity, photothermal evaluation. J Photochem Photobiol B 186:189–196
26. Hu W, Peng C, Luo W, Lv M, Li X, Li D, Huang Q, Fan C (2010) Graphene-based antibacterial paper. ACS Nano 4:4317–4323
27. Nanda SS, Yi DK, Kim K (2016) Study of antibacterial mechanism of graphene oxide using Raman spectroscopy. Sci Rep 6:28443
28. Liu S, Zeng TH, Hofmann M, Burcombe E, Wei J, Jiang R, Kong JC, Chen Y (2011) Antibacterial activity of graphite, graphite oxide, graphene oxide, and reduced graphene oxide: membrane and oxidative stress. ACS Nano 5:6971–6980
29. Kuila T, Bose S, Khanra P, Mishra AK, Kim NH, Lee JH (2012) A green approach for the reduction of graphene oxide by wild carrot root. Carbon 50:914–921
30. Thakur S, Karak N (2012) Green reduction of graphene oxide by aqueous phytoextracts. Carbon 50:5331–5339
31. Zhu C, Guo S, Fang Y, Dong S (2010) Reducing sugar: new functional molecules for the green synthesis of graphene nanosheets. J Am Chem Soc 4:2429–2437
32. Tran DNH, Kabiri S, Losic D (2014) A green approach for the reduction of graphene oxide nanosheets using non-aromatic amino acids. Carbon 76:193–202
33. Liu Y, Zhang Y, Ma G, Wang Z, Liu K, Liu H (2013) Ethylene glycol reduced graphene oxide/polypyrrole composite for supercapacitor. Electrochim Acta 88:519–525
34. Kamisan AI, Kamisan AS, Md Ali R, Tunku Kudin TI, Hassan OH, Halim NA, Yahya MZA (2015) Synthesis of graphene via green reduction of graphene oxide with simple sugars. Adv Mat Res 1107:542–546
35. Wang Y, Shi Z, Yin J (2011) Facile Synthesis of soluble graphene via a green reduction of graphene oxide in tea solution and its biocomposites. ACS Appl Mater Interfaces 3:1127–1133
36. Khosroshahi Z, Kharaziha M, Karimzadeh F, Allafchian A (2018) Green reduction of graphene oxide by ascorbic acid. AIP Conf Proc 1920:020009-1–020009-7
37. Mindivan F, Göktaş M (2018) Green synthesis of reduced graphene oxide (RGNO)/polyvinylchloride (PVC) composites and their structural characterization. Mater Res Forum LLC 8:143–151
38. Fernandez-Merino MJ, Guardia L, Paredes JI, Villar-Rodil S, Solis-Fernandez P, Martinez-Alonso A, Tascon JMD (2010) Vitamin C is an ideal substitute for hydrazine in the reduction of graphene oxide suspensions. J Phys Chem C 114:6426–6432
39. Guo Y, Sun X, Liu Y, Wang W, Qiu H, Gao J (2012) One pot preparation of reduced graphene oxide (RGO) or Au (Ag) nanoparticle-RGO hybrids using chitosan as a reducing and stabilizing agent and their use in methanol electrooxidation. Carbon 50:2513–2523
40. Yassin AY, Mohamed AR, Abdelrazek EM, Morsi MA, Abdelghany AM (2018) Structural investigation and enhancement of optical, electrical and thermal properties of poly (vinyl chloride-co-vinyl acetate-co-2-hydroxypropyl acrylate)/graphene oxide nanocomposites. J Mater Res Technol ın press
41. Yassin AY, Mohamed AR, Abdelghany AM, Abdelrazek EM (2018) Enhancement of dielectric properties and AC electrical conductivity of nanocomposite using poly (vinyl chloride-co-vinyl acetate-co-2-hydroxypropyl acrylate) filled with graphene oxide. J Mater Sci Mater Electron 29(18):15931–15945
42. Hummers WS, Offeman RE (1958) Preparation of graphitic oxide. J Am Chem Soc 6(80):1339
43. ASTM D 3822 (1997) Standard test method for tensile properties of single textile fibers. Am Soc Test Mater

44. Szabó T, Berkesi O, Dékány I (2005) DRIFT study of deuterium-exchanged graphite oxide. Carbon 43:3181–3194
45. Wang G, Wang B, Park J, Yang J, Shen X, Yao J (2009) Synthesis of enhanced hydrophilic and hydrophobic graphene oxide nanosheets by a solvothermal method. Carbon 47:68–72
46. Sun X, Liu Z, Welsher K, Robinson JT, Goodwin A, Zaric S, Dai H (2008) Nano-graphene oxide for cellular imaging and drug delivery. Nano Res 1:203–212
47. Pham TA, Choi BC, Jeong YT (2010) Facile covalent immobilization of cadmium sulfide quantum dots on graphene oxide nanosheets: preparation, characterization, and optical properties. Nanotechnology 21:465603
48. Zhang T, Zhang D (2011) Aqueous colloids of graphene oxide nanosheets by exfoliation of graphite oxide without ultrasonication. Bull Mater Sci 34(1):25–28
49. Ramesh S, Chai MF (2007) Conductivity, dielectric behavior and FTIR studies of high molecular weight poly (vinylchloride)—lithium triflate polymer electrolytes. Mater Sci Eng B 139:240–245
50. Chen J, Yao B, Li C, Shi G (2013) An improved Hummers method for eco-friendly synthesis of graphene oxide. Carbon 64:225–229
51. Marcano DC, Kosynkin DV, Berlin JM, Sinitskii A, Sun Z, Slesarev A, Alemany LB, Lu W, Tour JM (2010) Improved synthesis of graphene oxide. ACS Nano 4(8):4806–4814
52. Dreyer DR, Park S, Bielawski CW, Ruoff RS (2010) The chemistry of graphene oxide. Chem Soc Rev 39:228–240
53. Feng H, Li Y, Li J (2012) Strong reduced graphene oxide—polymer composites: hydrogels and wires. RSC Adv 2:6988–6993
54. Bao C, Song L, Xing W, Yuan B, Wilkie CA, Huang J, Guo Y, Hu Y (2012) Preparation of graphene by pressurized oxidation and multiplex reduction and its polymer nanocomposites by masterbatch-based melt blending. J Mater Chem 22:6088–6096
55. Mallakpour S, Sadeghzadeh R (2017) Facile and green methodology for surface-grafted Al_2O_3 nanoparticles with biocompatible molecules: preparation of the poly(vinyl alcohol)@poly(vinyl pyrrolidone)nanocomposites. Polym Adv Technol 28:1719–1729
56. Safarpour M, Khataee A, Vatanpour V (2015) Thin film nanocomposite reverse osmosis membrane modified by reduced graphene oxide/TiO_2 with improved desalination performance. J Membr Sci 489(1):43–54
57. Li D, Zhang B, Xuan F (2015) The sequestration of Sr(II) and Cs(I) from aqueous solutions by magnetic graphene oxides. J Mol Liq 209:508–514
58. Bora C, Bharali P, Baglari S, Dolui SK, Konwar BK (2013) Strong and conductive reduced graphene oxide/polyester resin composite films with improved mechanical strength, thermal stability and its antibacterial activity. Compos Sci Technol 87:1–7
59. Deshmukh K, Joshi GM (2014) Thermo-mechanical properties of poly (vinyl chloride)/graphene oxide as high performance nanocomposites. Polym Test 34:211–219
60. Khaleghi M, Didehban K, Shabanian M (2017) Effect of new melamine-terphetaldehyde resin modified graphene oxide on thermal and mechanical properties of PVC. Polym Test 63:382–391
61. Goumri M, Poilâne C, Ruterana P, Doudou BB, Wery J, Bakour A, Baitoul M (2017) Synthesis and characterization of nanocomposites films with graphene oxide and reduced graphene oxide nanosheets. Chin J Phys 55(2):412–422
62. Vadukumpully S, Paul J, Mahanta N, Valiyaveettil S (2011) Flexible conductive graphene/poly(vinyl chloride) composite thin films with high mechanical strength and thermal stability. Carbon 49:198–205
63. Yang S, Lei P, Shan Y, Zhang D (2018) Preparation and characterization of antibacterial electrospun chitosan/poly (vinyl alcohol)/graphene oxide composite nanofibrous membrane. Appl Surf Sci 435:832–840
64. O'Neill A, Bakirtzis D, Dixon D (2014) Polyamide 6/Graphene composites: the effect of in situ polymerisation on the structure and properties of graphene oxide and reduced graphene oxide. Eur Polym J 59:353–362
65. Li P, Chen X, Zeng J-B, Gan L, Wang M (2016) Enhancement of the interfacial interaction between poly(vinyl chloride) and zinc oxide modified reduced graphene oxide. RSC Adv 6:5784–5791
66. Liu S, Sun H, Suvorova A, Wang S (2013) One-pot hydrothermal synthesis of ZnO-reduced graphene oxide composites using Zn powders for enhanced photocatalysis. Chem Eng J 229:533–539
67. Awad WH, Beyer G, Benderly D, Ijdo WL, Songtipya P, Jimenez-Gasco MM, Manias E, Wilkie CA (2009) Material properties of nanoclay PVC composites. Polymer 50:1857–1867

68. Feng X, Xing W, Song L, Hu Y, Live KM (2015) TiO_2 loaded on graphene nanosheet as reinforcer and its effect on the thermal behaviors of poly (vinyl chloride). Chem Eng J 260:524–531
69. Ma F, Yuan N, Ding J (2013) The conductive network made up by the reduced graphene nanosheet/polyaniline/polyvinyl chloride. J Appl Polym Sci 38624:3870–3875
70. Duttagupta SP, Chen XL, Jenekhe SA, Fauchet PM (1997) Microhardness of porous silicon films and composites. Solid State Commun 101:33–37
71. Hasan M, Lee M (2014) Enhancement of the thermo-mechanical properties and efficacy of mixing technique in the preparation of graphene/PVC nanocomposites compared to carbon nanotubes/PVC. Proc Natl Sci Mater 24:579–587
72. Zheng Y-T, Cao D-R, Wang D-S, Chen J-J (2007) Study on the interface modification of bagasse fibre and the mechanical properties of its composite with PVC. Compos Part A 38:20–25
73. Li Y, Wang G, Liu S, Zhao S, Zhang K (2018) The preparation of Ni/GO composite foils and the enhancement effects of GO in mechanical properties. Compos B 135:43–48
74. Crespo JE, Sanchez L, Garcia D, Lopez C (2007) Containing rice husk fillers study of the mechanical and morphological properties of plasticized PVC composites. J Reinf Plast Compos 27(3):229–243